Process Biochemistry 49 (2014) 589–598

Contents lists available at ScienceDirect

Process Biochemistry

journal homepage: www.elsevier.com/locate/procbio

Plasma membrane behavior, oxidative damage, and defense mechanism in *Phanerochaete chrysosporium* under cadmium stress

Anwei Chen[a,b], Guangming Zeng[a,b,*], Guiqiu Chen[a,b,*], Liang Liu[a,b], Cui Shang[a,b], Xinjiang Hu[a,b], Lunhui Lu[a,b], Ming Chen[a,b], Ying Zhou[a,b], Qihua Zhang[a,b]

[a] College of Environmental Science and Engineering, Hunan University, Changsha 410082, PR China
[b] Key Laboratory of Environmental Biology and Pollution Control (Hunan University), Ministry of Education, Changsha 410082, PR China

ARTICLE INFO

Article history:
Received 23 October 2013
Received in revised form
23 December 2013
Accepted 17 January 2014
Available online 27 January 2014

Keywords:
Cadmium toxicity
Oxidative stress
Antioxidants
Phanerochaete chrysosporium
Extracellular crystal particle biosynthesis

ABSTRACT

Microorganisms are essential for maintaining ecosystem balance, and understanding their response to toxic pollutants is important in assessing the potential environmental impacts of such releases. In this study, the response to the heavy metal cadmium and the potential defense or adaptive mechanisms of the widely used white-rot fungus, *Phanerochaete chrysosporium*, were investigated. The results indicated that cadmium causes plasma membrane damage, including rigidification of lipids, a decrease in H^+-ATPase activity, and lipid peroxidation. The cellular death may be mediated by oxidative stress with mitochondria membrane potential (MMP) breakdown and reactive oxygen species (ROS) formation. Parts of the cells were able to survive by activating antioxidant defense systems (antioxidant agents and enzymes). Extracellular synthesis of cadmium crystal particles was observed after exposure to dissolved cadmium ion, which is probably another detoxification mechanism in which the dissolved metal is precipitated, thus reducing its bioavailability and toxicity. These physiological responses of *P. chrysosporium* to cadmium together with the defense mechanisms can provide useful information for the development of fungal-based technologies to reduce the toxic effects of cadmium.

1. Introduction

The use of microorganisms in bioremediation has been extensively studied. *Phanerochaete chrysosporium*, a white-rot fungus, has been found to be efficient in treating wastewater containing heavy metals and toxic organic pollutants because of its unique ability to degrade xenobiotics and bioabsorb heavy metals [1–3]. However, the ability of *P. chrysosporium* to remove pollutants varies substantially with the types of pollutants and reaction conditions [3–5]. Moreover, its colonization and bioactivity depend largely on the types of pollutants and reaction conditions [1,6].

Generally, the objects disposed by *P. chrysosporium* are often toxic. For example, cadmium, a non-essential heavy metal widely present in the environment, is one of the most toxic environmental pollutants to all living cells [7]. Extensive studies have revealed that cadmium is toxic to aquatic plants at all levels—cellular, physiological, biochemical, and molecular [8]. The uptake and accumulation of cadmium in plant usually causes ROS burst by displacing Fe from proteins and inhibiting the electron transport chain in the mitochondria, as well as by inhibiting antioxidative systems in living cells. The excess ROS generated reacts with lipids, proteins, and pigments, and finally results in membrane damage and enzyme inactivation [9,10]. Other symptoms of cadmium toxicity include growth inhibition, proteins and DNA oxidation, and ultrastructural changes [8,11]. In the microorganism bioremediation research field, cadmium is also regarded as one of the most toxic heavy metals. Our previous study also demonstrated cadmium reduced protein production and enzymatic activities (lignin peroxidase and manganese peroxidase) of *P. chrysosporium* [3].

The toxic effects of pollutants affect microbial physiological changes, bioactivity, and colonization, resulting in decreased treatment ability [6] and limiting the development and popularization of biological treatment technologies. Therefore, understanding the response of *P. chrysosporium* to toxic pollutants stress in the medium is essential. Previous studies on cadmium removal using *P. chrysosporium* have provided some useful information on the relationship between fungal activities and cadmium removal [12,13]. Our previous study also reported that *P. chrysosporium* can bind Cd^{2+} ions by its mycelium and extracellular polymeric substances and remove them from wastewater [5]. However, information on

* Corresponding author at: College of Environmental Science and Engineering, Hunan University, Changsha 410082, PR China. Tel.: +86 731 88822829; fax: +86 731 88823701.
E-mail addresses: zgming@hnu.edu.cn (G. Zeng), gqchen@hnu.edu.cn (G. Chen).

1359-5113/$ – see front matter © 2014 Elsevier Ltd. All rights reserved.
http://dx.doi.org/10.1016/j.procbio.2014.01.014

the physiological responses of *P. chrysosporium* under cadmium stress is still limited. In particular, the effects of cadmium stress on the resistance, and adaptive responses of *P. chrysosporium* have not yet been reported in the literature.

In view of this, the main purpose of the present study was to explore cadmium toxicity in *P. chrysosporium* using physiological measurements. This study investigated the oxidative damage induced by cadmium and the defense mechanism of *P. chrysosporium* against these stresses. To assess physiological responses, we investigated plasma membrane fluidity, H^+-ATPase variation, and oxidative damage following exposure to cadmium because these variations can be used as indicators of microbial fitness and survival [14]. In addition, the antioxidative responses or defense mechanisms were evaluated.

2. Materials and methods

2.1. Strain and treatment

The *P. chrysosporium* strain BKMF-1767 (CCTCC AF96007) used in this study was obtained from the China Center for Type Culture Collection (Wuhan, China). Stock cultures were maintained on malt extract agar slants at 4 °C. Spores were gently scraped from the agar surface and blended in sterile distilled water to obtain a spore suspension. The spore concentration was adjusted to 2.0×10^6 spores/ml. Aqueous suspensions of fungal spores were inoculated into Kirk's liquid culture medium [15] in 500-ml Erlenmeyer flasks. Flasks containing 8×10^6 spores were incubated at 37 °C in an incubator. After 2 days of growth in liquid culture, the mycelia were treated with various concentrations of $Cd(NO_3)_2$ for 24 h. The mycelia were then harvested and washed twice with ultrapure water for further analysis. All chemicals used in this study were at least of analytical reagent grade.

2.2. Plasma membrane H^+-ATPase activity assay

The plasma membrane was obtained according to the methods described by Perlin et al. [16]. Plasma membrane H^+-ATPase activity was determined as the amount of P_i released by hydrolysis of ATP in the reaction mixture [17]. Released phosphate comes from the hydrolysis of ATP by ATPase in plasma membrane, as well as by apyrases and alkaline phosphatases, which are resistant to the inhibitors for mitochondrial ATPase (sodium azide), vacuolar ATPase (potassium nitrate), acid phosphatase (ammonium molybdate) and plasma membrane ATPase (Na_3VO_4). Accordingly, H^+-ATPase activity in plasma membrane was determined as the difference between the activities in the presence and absence of the inhibitor Na_3VO_4. Plasma membrane H^+-ATPase activity was measured using 5 ml disposable plastic tubes with 24 μl of purified plasma membrane and 500 μl of reaction mixture containing 50 mM 2-(N-morpholino)ethanesulfonic acid adjusted to pH 5.7 with Tris, 5 mM magnesium sulfate, 50 mM potassium nitrate, 5 mM sodium azide, 0.2 mM ammonium molybdate, and 1 μl of water or inhibitor (0.1 M Na_3VO_4). After 3 min of incubation at 30 °C, the assay was started by adding 10 μl of 0.1 M Na_2ATP. Color was developed for 10 min, and the absorbance at 690 nm was measured in a UV–vis spectrophotometer (Model UV-2550, Shimadzu Company, Tokyo, Japan). A calibration curve for phosphate was obtained for amounts of phosphate from 0.5 to 0.01 μmol supplied in a 0.1 M solution of Na_2HPO_4 as standard. One unit of activity corresponded to 1 μmol P_i released per min. The specific activity was expressed in units per g protein.

The protein concentration was determined by colorimetrically using a UV–vis spectrophotometer (Model UV-2550; Shimadzu Company, Tokyo, Japan) at 595 nm according to the method of Bradford [18] using bovine serum albumin as a standard.

2.3. Membrane fluidity determination

Fluidity of the plasma membrane was determined according to a previously described method [19]. Briefly, 282 mM mannitol (pH 7.2) and 50 μM 8-anilino-1-naphthalene-sulfonic acid (ANS) were added into the assay medium. An appropriate volume of plasma membrane preparation was then added to the medium to ensure that the amount of protein was identical in every determination. After 1 min of ANS addition and mixing, the fluorescence intensity was recorded at 22 °C using a fluorescence spectrometer (FluoroMax-4; Horiba Scientific, Tokyo, Japan). Fluorescence intensity was inversely proportional to membrane fluidity.

2.4. Cell viability assay

Cell viability was assessed using the MTT assay according to Luo et al. [20] with some modifications. MTT is a yellow water-soluble tetrazolium dye that is reduced by living cells to a water-insoluble purple formazan. The conversion of the MTT into purple formazan occurs only in living cells with active mitochondria and is directly proportional to the number of viable cells. Briefly, 0.2 g *P. chrysosporium* pellets were mixed with 1 ml MTT solution (5 g/l) and incubated at 50 °C. The reaction was stopped by adding 0.5 ml hydrochloric acid (1 M) to the mixture. The mixture was centrifuged (10,000 × g, 5 min), the supernatant was discarded, and the pellets were agitated in 6 ml propan-2-ol for 2.5 h. The centrifugation process was repeated and the absorbance of the supernatant was recorded at 534 nm. In the test, an antioxidant agent (vitamin C, 0.1 mM) was used to explore the compensating effects against to cadmium toxicity.

2.5. ROS generation

The degree of ROS generation induced by cadmium was determined using a fluorometric indicator, 2,7-dichlorodihydrofluoresceindiacetate (H_2DCF-DA), as previously described [21]. H_2DCF-DA could be transformed into 2,7-dichlorodihydrofluorescein (H_2DCF) by intracellular esterase if they enter cells. When intracellular ROS generated, 2,7-dichlorofluorescein (DCF) would be converted from H_2DCF. Thus we measured the fluorescence intensity of DCF, which indicated the extent of ROS generation. Before cadmium exposure, the cells were incubated with H_2DCF-DA (5 μM) in incubation medium for 2 h. The H_2DCF-DA was then removed, and the mycelia were treated with the indicated cadmium concentrations. The medium was then removed, and the cells were washed with phosphate-buffered saline (PBS). Fluorescence was measured using a fluorescence spectrometer (FluoroMax-4; Horiba Scientific, Tokyo, Japan) with filters for excitation at 485 nm and emission at 525 nm.

2.6. Membrane lipid peroxidation and integrity assay

The cadmium-induced membrane liquid peroxidation was estimated by measuring the concentrations of malondialdehyde (MDA), which is a cytotoxic product of lipid peroxidation and an indicator of free radical production and consequent tissue damage. The harvested *P. chrysosporium* were homogenized in 10% trichloroacetic acid and centrifuged at 10,000 × g for 15 min. The supernatant was boiled with thiobarbituric acid for 20 min. The heated supernatant was centrifuged at 5000 rpm for 5 min, and the absorbance was measured at 532 and 600 nm [22].

The membrane integrity of the cells exposed to cadmium stress was measured using the fluorescent dye propidium iodide (PI). When the cell membrane was intact, PI could not move across the membrane to intercalate with nucleic acids. However, PI could enter cells and stain nucleic acids if the integrity of the cell membrane was compromised when the cells were under stress [23]. The PI stock solution (1 mg/ml) was prepared by dissolving PI into PBS and stored at 4 °C before use. The stain was diluted with PBS to a final concentration of 50 μg/ml, and samples were immersed for 20 min and then rinsed in PBS before imaging under a fluorescence microscope (BX-61; Olympus, Tokyo, Japan).

2.7. Mitochondrial properties

Mitochondrial fractions were isolated using the method of successive differential centrifugation [24]. *P. chrysosporium* cells were homogenized in an ice-chilled extraction medium consisting of 0.4 M mannitol, 50 Mm Tris–HCl, 10 mM EDTA, 0.1% (w/v) bovine serum albumin, and 0.05% (v/v) β-mercaptoethanol at pH 7.4. The homogenate was centrifuged at 600 × *g* for 10 min, and the supernatant was re-centrifuged at 10,000 × *g* for 30 min at 4 °C. The sediment was then washed twice with the above extraction medium for further use.

The freshly prepared mitochondria were resuspended in an assay medium containing 0.25 M sucrose, 2 mM HEPES, 0.5 mM KH_2PO_4, and 4.2 mM sodium succinate at pH 7.4. The mitochondrial membrane potential (MMP) was detected using a specific MMP-dependent fluorescent dye (Rhodamine 123) [25]. For steady measurements, mitochondrial fractions were incubated with Rh 123 at a final concentration of 1 mg/ml for 30 min at 25 °C in the dark. Mitochondrial fractions were then harvested and washed twice with the above extraction medium. The Rh 123 fluorescent images were captured using a spectrofluorometer (excitation, 505 nm; emission, 510–530 nm). The membrane permeability and cytochrome *c*/*a* ratio of the isolated mitochondria were measured following Tonshin et al. [26].

2.8. Antioxidant analyses

The antioxidative enzyme activity was measured by harvesting the cells by centrifugation and homogenization in 0.05 M PBS (pH 7.8). The homogenate was centrifuged at 15,000 rpm at 4 °C, and the supernatant was used for the enzyme assay. The superoxide dismutase (SOD) and catalase (CAT) activities were measured as previously described [27]. Peroxidase (POD) activity was detected by monitoring the oxidation of guaiacol at A_{470} nm. The final reaction mixture contained 1.0 ml 0.05 M PBS (pH 7.0), 0.8 ml 0.2% guaiacol, and 1.0 ml 0.3% H_2O_2. The reaction was initiated by 0.2 ml enzyme sample. One unit of POD activity was defined as the increased absorbance of 0.01 at A_{470} nm/min under assay conditions.

Glutathione content was determined using 5,5-V-dithiobis-(2-nitrobenzoic acid)-glutathione disulfide according to the method described by Rehman and Anjum [28]. Briefly, the mycelia were rinsed with phosphate buffer (0.1 M, pH 7.0) plus 0.5 mM EDTA and sonicated. The sample was sonicated for 3 s in intervals of 8 s with the output power of 400 W. The sonication was carried out for a total time of 5 min for each sample. The suspension was centrifuged at 14,000 × *g* for 10 min, and the supernatant was used for estimating the concentration of glutathione. Reduced glutathione (GSH) was estimated by adding 2.0 ml of reaction buffer to 0.5 ml of the above aliquot, followed by addition of 0.5 ml of 3 mM 5-dithio-bis-(2-nitrobenzoic acid). After 5 min, absorbance was recorded at 412 nm. In the same tube, 100 μl of 0.4 mM NADPH and 2 μl glutathione reductase were added. After 20 min, optical density was measured at 412 nm for the determination of total glutathione. The amount of glutathione disulfide (GSSG) was calculated by subtracting GSH from total concentrations.

2.9. SEM and EDX analyses

A scanning electron microscope (SEM) was used to obtain surface information and examine the morphology of *P. chrysosporium*. The samples exposed to $Cd(NO_3)_2$ for 24 h were harvested by filtration, washed with distilled water, and then dried in a freeze dryer (FD-1; Boyikang, Beijing, China). The dry mycelial pellets were imaged using an SEM (FEI QUANTA-200; Holland FEI Company, Holland) equipped with an energy dispersive X-ray (EDX). Micrographs were obtained and the corresponding EDX spectra were recorded.

2.10. TEM and XRD analyses

The mycelium pellets (exposed to cadmium for 24 h) were harvested by filtration and washed with distilled water. The cadmium crystal particles still attached to the mycelia were dispersed in water by ultrasonication. For TEM, a drop of aqueous solution containing cadmium crystal particles was placed on a carbon-coated copper grid and air-dried. Transmission electron micrographs were obtained using a TEM (H-800, Hitachi, Japan). For XRD analysis, the freeze-dried mycelium pellets (exposed to cadmium for 24 h) embedded with cadmium crystal particles were powdered. The pattern was recorded using an automatic X-ray diffractometer (D/MAX2550VB+, Rigaku Corporation, Japan).

2.11. Data analysis

Data are expressed as the means ± SE of three independent experiments. Statistical evaluation of the results was determined by Tukey post hoc test. Differences were considered to be significant at $p < 0.05$.

3. Results

3.1. Action of cadmium on cellular viability

The effect of cadmium exposure on the viability of *P. chrysosporium* was investigated by incubating *P. chrysosporium* with different concentrations of cadmium (1–500 μM) for 24 h. The results showed that cadmium reduced cell viability even at the lowest concentration (Fig. 1). This trend was particularly noticeable at higher cadmium concentrations (50–500 μM). Death occurred in approximately 74% of the total cells at higher cadmium concentration (100 or 500 μM). The death induced by 100 μM cadmium was reversed, in part, by adding vitamin C, an antioxidant agent.

3.2. Changes in plasma membrane fluidity and H^+-ATPase activity

The membrane fluidity of *P. chrysosporium* under cadmium stress was estimated by determining the fluorescence intensity of the probe (ANS) detected in the plasma membranes. A lower intensity indicates faster molecular motion, indicating higher plasma membrane fluidity. As shown in Fig. 2A, the membrane fluidity decreased with an increase in cadmium concentration (indicated by the high fluorescence intensity). Maximum fluorescence intensity was observed at the highest cadmium concentration, which was approximately 6.8-fold that of the control. The fluorescence spectrum of each sample is shown in Fig. S1 (Supplementary Fig. S1).

Similar to membrane fluidity, plasma membrane H^+-ATPase activity decreased in a concentration-dependent manner after exposure to cadmium (Fig. 2B). Higher concentrations of cadmium

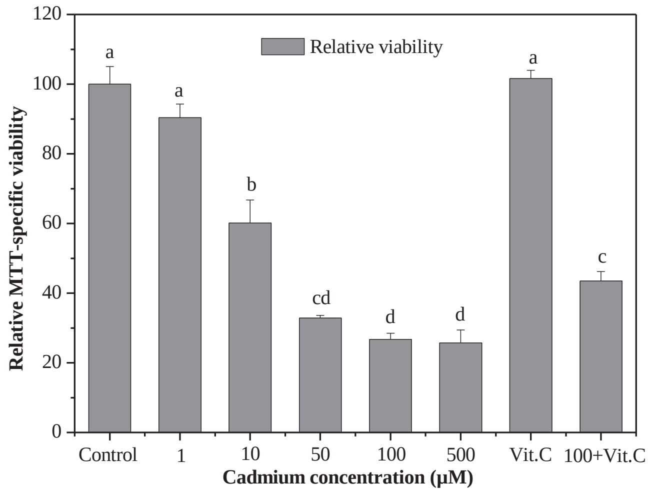

Fig. 1. Effect of cadmium exposure on the cell viability of *P. chrysosporium*. "Vit. C" refers to vitamin C. Columns labeled with different letters are significantly different at $p < 0.05$.

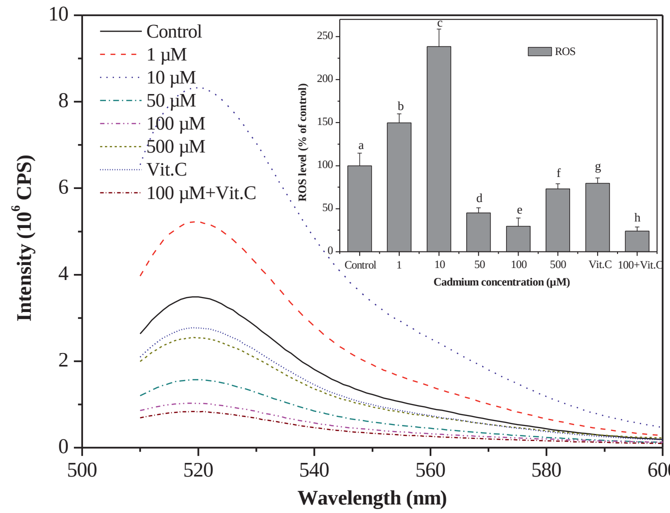

Fig. 3. Fluorescence intensity reflects ROS generation of *P. chrysosporium* after cadmium exposure. Figure inset shows the ROS level of each treatment respect to control. "Vit. C" refers to vitamin C. Different letters mean significance of difference between the treatments ($P < 0.05$).

caused distinct inhibition of H^+-ATPase activity. The greatest inhibition of ATP hydrolysis (as much as 90%) was observed in plasma membranes treated with 500 μM cadmium, while 1 μM cadmium induced 25% inhibition of ATP hydrolysis.

3.3. ROS generation and membrane damage

Results of the H_2DCF-DA dye test showed that ROS formation was a significant response after cadmium exposure (Fig. 3). The intracellular ROS increased with cadmium concentration when concentrations remained low (1–10 μM). However, the intracellular ROS levels in *P. chrysosporium* treated with higher cadmium concentrations (50–500 μM) was even lower relative to that of the control. Interestingly, ROS generation was partly revised by addition of vitamin C under the same cadmium treatment conditions.

Lipid peroxidation was evaluated by measuring the MDA level as described in Section 2.6. Fig. 4 shows the representative MDA content in *P. chrysosporium* cells under various cadmium treatments. The elevated MDA levels suggest that metal ions stimulate the free radical-generating capacity of the microorganism; however, this elevation was not always observed. At lower concentrations (1–10 μM), cadmium increased the MDA content after exposure for 24 h. A significant increase in MDA content was particularly noted in the cells treated with the lowest cadmium concentration (1 μM). On further increasing the cadmium concentration, however, the MDA content became lower than that of the control. Therefore, two other control groups (*P. chrysosporium* exposed to cadmium for 2 h at the incubation time of 2 days and 3 days, respectively) were used to explore the difference (Fig. 4). Elevated MDA levels were observed at higher cadmium concentration (100–500 μM) in the two control groups compared to that of a lower cadmium concentration (0–50 μM). The results from these three groups coupled with the cell viability result shown in Fig. 1 suggested that long-term exposure to high concentrations of cadmium led to overproduction of ROS, causing chronic damage and cell death.

The damage and integrity of the plasma membrane was determined using the membrane permeability stain (PI stain). A PI-positive nucleus strongly indicates loss of membrane integrity.

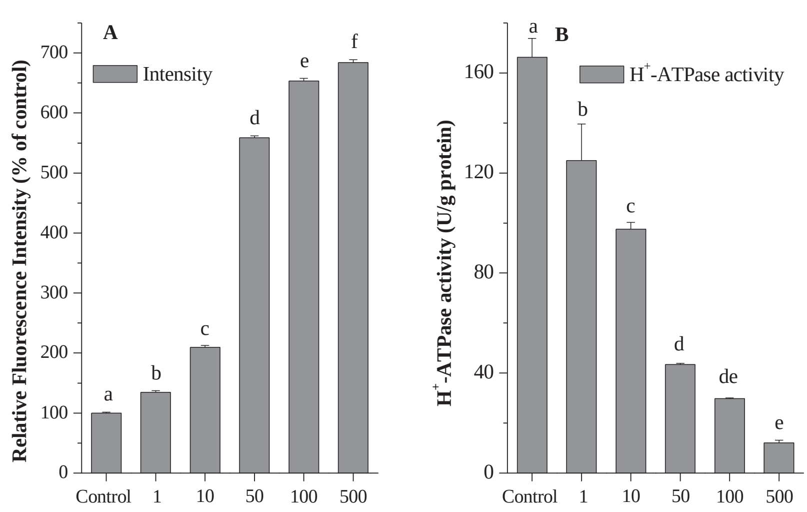

Fig. 2. (A) Fluorescence intensity representing the plasma membrane fluidity of *P. chrysosporium* exposed to various cadmium concentration. Fluorescence intensity was inversely proportional to membrane fluidity. (B) Plasma membrane H^+-ATPase activity of *P. chrysosporium* after exposed to the indicated cadmium concentration for 24 h. Different letters denote significant differences between treatments ($p < 0.05$).

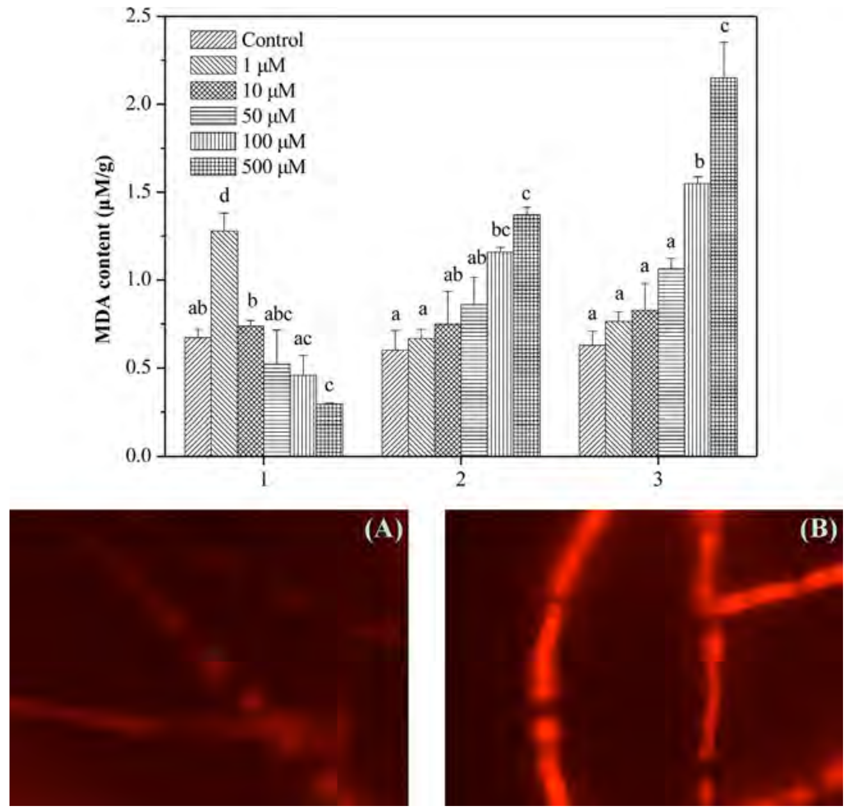

Fig. 4. Cadmium induced MDA content in *P. chrysosporium*. (1) a 2-day-old culture was treated with cadmium and further cultivated for 24 h; (2) a 2-day-old culture was treated with cadmium and further cultivated for 2 h; (3) a 3-day-old culture was treated with cadmium and further cultivated for 2 h. Images reflect the plasma membrane intensity of *P. chrysosporium* cell for (A) control and (B) 100 μM cadmium for 24 h. Different letters indicate significant differences between the treatments ($p < 0.05$).

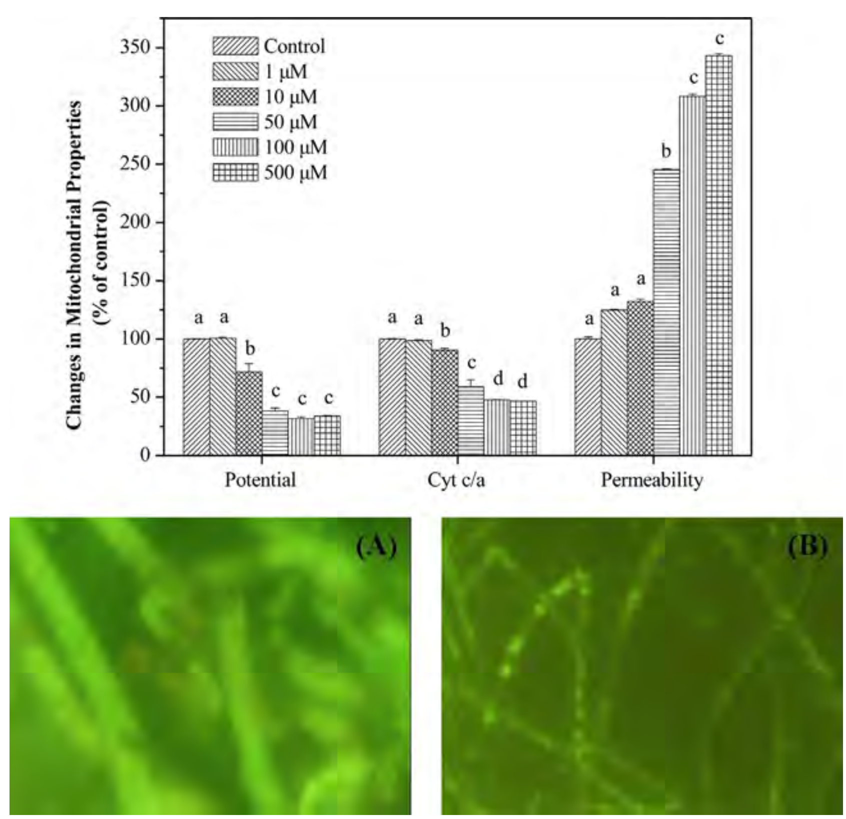

Fig. 5. The bar graph shows mitochondrial properties changes induced by cadmium. Images reflect the mitochondrial membrane potential alteration of *P. chrysosporium* cell for (A) control and (B) 100 μM cadmium for 24 h. Different letters indicate significant differences between the treatments ($p < 0.05$).

The Images in Fig. 4 represent that *P. chrysosporium* cell showed stronger red fluorescence after exposure to cadmium for 24 h compared with control (un-exposed), which indicates a loss of membrane integrity seriously. Consistent with the cell viability assay, ROS formation, and lipid peroxidation, the results of PI staining showed that exposure to 100 μM cadmium for 24 h led to obvious cell damage and death (Fig. 4).

3.4. Alteration of mitochondrial properties

As shown in Fig. 5, cadmium reduced the MMP level (the bar graph). This phenomenon was particularly observed when cells were exposed to high concentrations of cadmium. The images show that living cells in the control were strongly stained by Rh-123 (high MMP), whereas weak Rh-123 staining (low MMP) was observed in the cells treated with 100 μM cadmium for 24 h. Concomitantly, cadmium-induced cytochrome *c* (Cyt *c*) release from mitochondria was also observed, which was evident from the decrease in the cytochrome *c*/*a* ratio. The mitochondrial membrane permeability markedly increased after cadmium exposure (Fig. 5).

3.5. Quantification of antioxidants

Antioxidant enzymes have been considered the first line of defense in response to oxidative stress [29]. In the present study, we monitored the activities of SOD, CAT, and POD, which have been reported to be important in the oxidative stress defense in fungi [30]. As shown in Fig. 6, the activity of SOD in *P. chrysosporium* exposed to cadmium was similar to that of MDA, as described above. When cells were exposed to cadmium for 24 h, enhanced SOD activity was observed only at lower cadmium concentrations (1–10 μM). When cells were exposed for only a short time (2 h), enhanced SOD activity was noted at all tested cadmium concentrations. The CAT and POD activities were lower than those of the control after 24 h of cadmium exposure, except in the case of the lowest cadmium concentration (1 μM; Fig. 7). The SOD, CAT, and POD activities were significantly responsive to the cadmium concentration in the medium. Generally, a lower concentration of cadmium or short-time exposure increased the activities of these enzymes. In contrast, addition of cadmium at larger lethal doses or exposure over a long period failed to induce these enzymes. Therefore, the induction of antioxidant enzyme activities is essential for cells to acquire the ability to overcome oxidative stress to some extent.

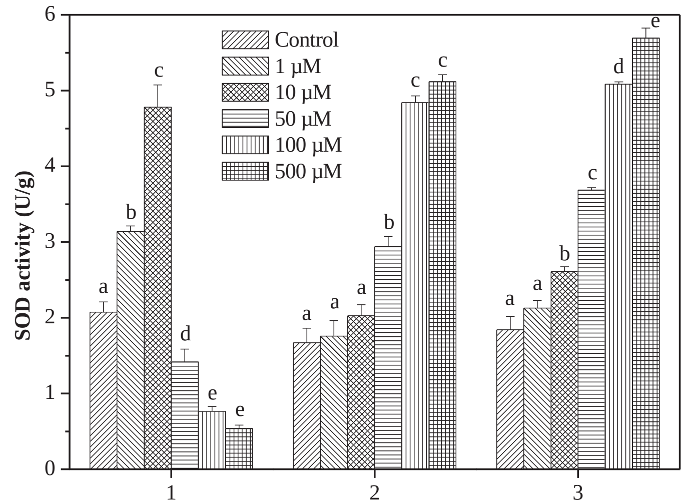

Fig. 6. Cadmium induced SOD activity in *P. chrysosporium*. (1) a 2-day-old culture was treated with cadmium and further cultivated for 24 h; (2) a 2-day-old culture was treated with cadmium and further cultivated for 2 h; (3) a 3-day-old culture was treated with cadmium and further cultivated for 2 h. Different letters indicate significant differences between the treatments ($p < 0.05$).

The changes in GSH and GSSG in response to cadmium exposure were also evaluated (Fig. 8). The concentrations of GSH increased from 72.8 μM/g protein to 110.1 μM/g protein at cadmium concentration from 0 μM to 50 μM, and changed little with further increases in cadmium concentration. However, an opposite trend was observed for GSSG. The GSH/GSSG ratio increased with increasing cadmium concentrations from 1 to 10 μM, and then began to decline with further increases in cadmium concentrations.

3.6. Extracellular biosynthesis of metallic crystal particles

SEM images of the native and cadmium-treated fungi are shown in Fig. 9. The surface of the native fungus was smooth and clear, without any adsorbed particles (Fig. 9A). The mycelium after

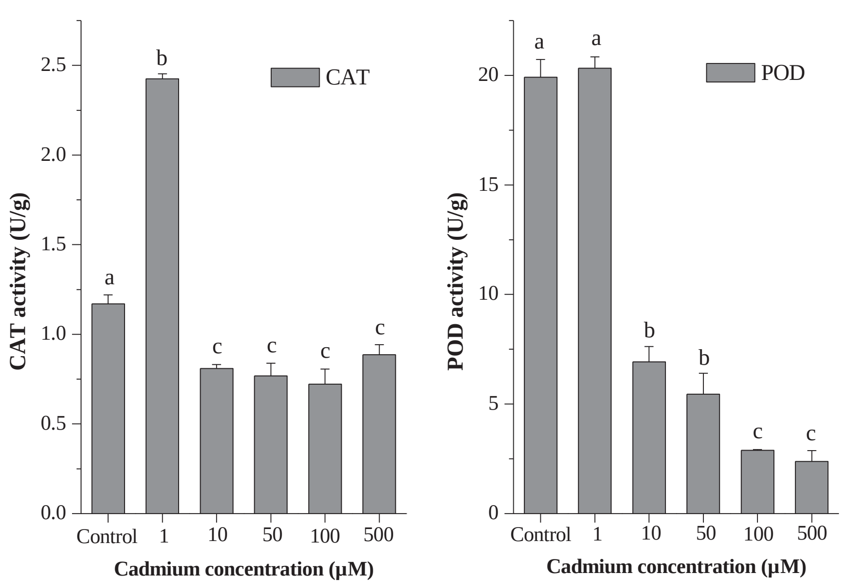

Fig. 7. The variation of CAT and POD activities in *P. chrysosporium* after exposure to cadmium for 24 h. Different letters indicate significant differences between the treatments ($p < 0.05$).

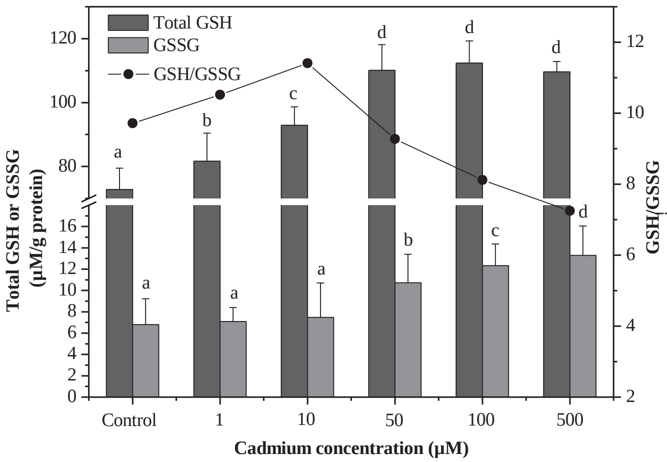

Fig. 8. Effect of cadmium exposure on the GSH and GSSG in *P. chrysosporium*. Different letters indicate significant differences between the treatments ($p < 0.05$).

incubation with cadmium was very different from that before incubation. The outline of the mycelium was not clear, and a large quantity of cadmium adhered to the surface of the mycelium, which appeared as many particles indicated by red arrows in Fig. 9B and C.

The EDX spectrum was used to analyze the elemental composition of the particles as indicated in Fig. 9C. The obvious cadmium peak in Fig. 9D suggests binding of cadmium ions to the surface of the biomass.

In order to further study the physicochemical properties of the particles observed in Fig. 9, TEM and XRD were used to clarify the characteristics. The TEM image (Fig. 10) shows that the cadmium particles were not uniform in size and shape. Some aggregation of the particles could also be observed. This could be related to the preparation technique that deposited the particles onto the copper grid. The average size of the particles estimated from the image was in the 10–30 nm range, which does not agree with the size estimated by SEM (Fig. 9C and D). This phenomenon shows that the particles seen in SEM pictures are probably clusters of several small particles with different sizes. As discussed, amino acids or proteins might play a role in this aggregation process. Further studies were carried out using XRD, an effective method for investigating the microstructure of crystalline or amorphous materials, to confirm the crystalline nature of the coarsened particles. The XRD pattern obtained is shown in Fig. 11. The XRD pattern exhibits four intense peaks at 2θ values of 26.98°, 31.25°, 44.78°, and 53.06°, which could be indexed to the (1 1 1), (2 0 0), (2 2 0), and (3 1 1) facets of the cubic phase CdS, respectively (JCPDS Powder Diffraction File no. 65-8873). The PDF card indicated that the crystal particles were

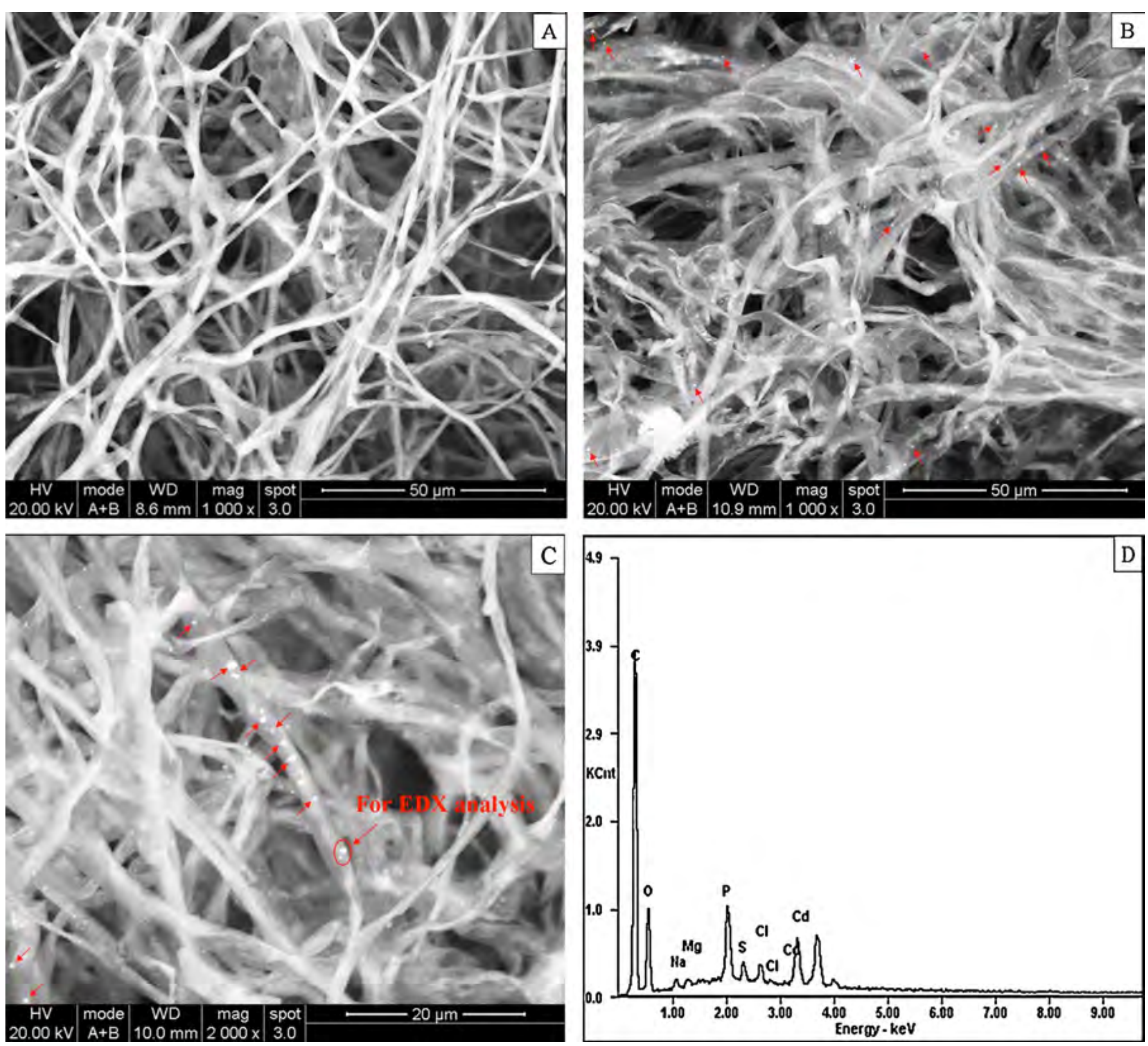

Fig. 9. SEM-EDX images show biosynthesis of cadmium crystal particles by *P. chrysosporium* during exposure to 0.1 mM $Cd(NO_3)_2$. Panel A show a SEM image of native mycelium; panel B (×1000) and C (×2000) shows a SEM image of *P. chrysosporium* mycelium and the biogenic crystal particles, pointed by red arrows; panel D depicts the EDX spectrum of the crystal particles in the image as indicated.

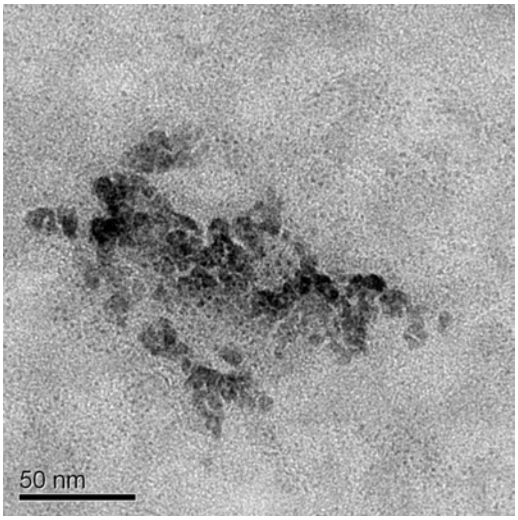

Fig. 10. Transmission electron micrographs of cadmium crystal particles with scale bar 50 nm.

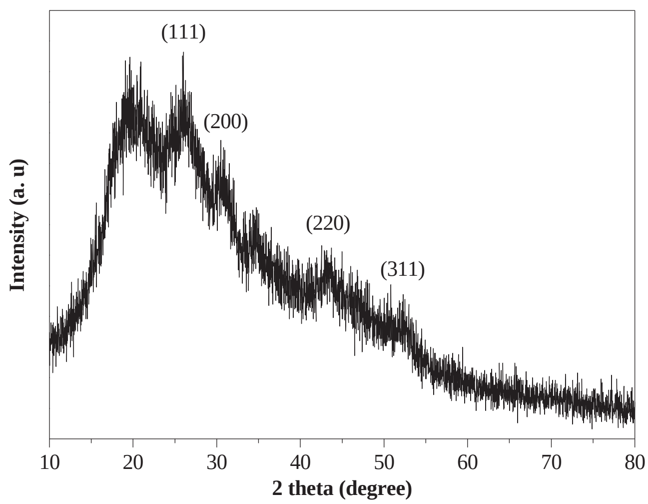

Fig. 11. XRD pattern of fungus sample impregnated with cadmium crystal particles.

in line with the face centered cubic crystal lattice having unit cell parameters: $a = b = c = 5.720$ belonging to space group Fm-3m (225). These results indicate that the cadmium-binding particles observed in this study were extracellular biosynthesis of cadmium crystal particles.

4. Discussion

4.1. Cadmium-induced oxidative damage and cell death

The plasma membrane is the first live line of defense against changes in physicochemical parameters; therefore, its integrity and functionality is of the utmost importance [14]. It can be considered the first “living” structure that is a target for heavy metal toxicity [31]. The present results of the effects on plasma membrane fluidity and H^+-ATPase activity support the view that the immediate target of Cd^{2+} is the cell membrane. In contrast to the control, the plasma membrane of the cadmium-treated group showed rigidification. Such damage could result from various mechanisms, including oxidation and cross-linking of protein thiols, inhibition of key membrane proteins such as H^+-ATPase, or changes in the composition of membrane lipids [31]. Reduction in the H^+-ATPase activity in the plasma membrane by cadmium treatment is consistent with this view. The direct effects of cadmium treatments on the lipid composition of membranes have been reported [32], and these might directly impact membrane permeability. Our study also proved that mitochondrial membrane permeability markedly increased after cadmium exposure (Fig. 5). These results suggest that cadmium produces changes in the fatty acid composition of the phospholipid fraction of the plasma membrane. However, changes in the fluidity of the plasma membrane after cadmium treatment cannot be attributed solely to changes in the fatty acid composition because the presence of cadmium-binding proteins has been reported, and this increase in rigidity might be a consequence of complex protein–lipid interactions in the plasma membrane [33].

The H^+-ATPase activity decreased with increasing cadmium concentrations. This was probably attributable to an alteration in membrane fluidity and lipid composition, the binding of Cd^{2+} to the —SH groups of the proteins, or Ca^{2+} replacement at essential sites of cell membranes [34]. The interaction between cadmium and membrane constituents such as lipids and/or proteins might result in the alteration of membrane fluidity which, in turn, affects the activities of membrane-bound enzymes [35]. H^+-ATPase is the only proton pump operating in the plasma membrane and plays a central role in the regulation of ion homeostasis. Ion transport across the plasmalemma is known to be dependent on the electrochemical gradient generated by plasma membrane H^+-ATPase; therefore, regulation of this enzyme could play an important role under cadmium stress conditions.

The cell viability analysis showed that cadmium exposure induced cellular death, which was partially reversed by vitamin C (an antioxidant agent). Previous studies revealed that vitamin C exhibited a beneficial role in the alleviation of cadmium toxicity through mitigating cadmium induced oxidative stress [36,37]. Vitamin C scavenges ROS by rapid electron transfer and there by acts as an important antioxidant defence against oxidative damage [38]. Thus, the presence of vitamin C partially mitigated cadmium induced cell death. The results also indicated that cadmium induces cell death in *P. chrysosporium* via the induction of ROS, eventually leading to oxidative stress. Cadmium at lower concentrations (1–10 μM) induced ROS generation, compared to that in the control (Fig. 3). The induction of ROS in cells could be mediated by alterations in the mitochondria, because cadmium is known to breakdown MMP. The breakdown of mitochondrial potentials were evident at doses of 10 and 500 μM cadmium, while ROS formation was detected at lower doses (1–10 μM). These results most probably indicate that ROS formation occurs or is detectable before the toxic effects on mitochondrial function that lead to the breakdown of mitochondrial potentials. Similar results were observed by Lópze et al. [21] in cortical neurons. There was a remarkable decrease in cell viability accompanied by mitochondria membrane-potential breakdown at higher cadmium concentrations. The decrease in Cyt *c*/*a* and increase in mitochondria membrane permeability indicate mitochondrial membrane breakdown. Cyt *c* is released after mitochondrial membrane permeabilization and leads to the induction of apoptosis [39].

Moreover, cadmium inhibits the mitochondrial electron-transfer chain, leading to the accumulation of semi-ubiquinone, which enables it to transfer one electron (e^-) to molecular oxygen to form superoxide radicals [40]. The free radical production, in turn, leads to lipid peroxidation [41]. The data in Fig. 4 indicate that this oxidative stress induced by cadmium is manifested by two effects: concentration- and time-dependent effects. For short-term exposure (2 h), the extent of lipid peroxidation increased with increases in cadmium concentration. Long-term exposure of *P. chrysosporium* under higher cadmium concentrations resulted in an even lower MDA level in the cells, which might be due to the sharp decrease in cell viability. Exposure of cells to high cadmium concentrations resulted in the accumulation of ROS; however, when the ROS levels exceeded the ability of *P. chrysosporium* to adapt, cellular damage occurred, resulting in cell death and lysis and decreased MDA detection [42].

4.2. The defense mechanism

The generation of cadmium-induced ROS stimulated the production of antioxidant agents and enzymes to protect cellular components from damage. Our results showed that the changes in SOD activity in *P. chrysosporium* exposed to cadmium exposure were similar to those of MDA content. SOD activity was well correlated with MDA levels ($r_1^2 = 0.972$ and $r_2^2 = 0.976$) (Supplementary Fig. S2) at cadmium concentrations from 1 to 100 μM under short-term exposure (2 h) after incubation of cells for 48 h and 72 h. However, when the ROS levels exceeded the ability of the antioxidant system to cope with them, cellular damage occurred, indicated by the lower SOD activity and MDA level at higher cadmium concentration exposure for 24 h compared to that in the control. The SOD and CAT activities at a cadmium concentration of 1 μM were higher than those of the control, and the other tested concentrations suggested that some parts of cells was resistant to cadmium. Basha and Rani [43] suggested that upregulation of enzyme production might be a defense mechanism, providing a first line of defense against cadmium toxicity before the induction of metallothionein synthesis.

In addition to the above antioxidant enzymes, the intracellular concentration of GSSG increased with increase in cadmium concentration from 10 μM to 500 μM, and the GSH/GSSG ratio exhibited a bell-shaped response at a maximum dose of 10 μM cadmium. This is most probably because of the depletion of reduced glutathione in the reaction of ROS and the rapid increase in GSSG [44], which indicates the importance of glutathione in detoxification and the potential of *P. chrysosporium* to tolerate cadmium stress. Our results are in accordance with those of Gharieb and Gadd [45] who reported direct evidence for the involvement of glutathione in cadmium detoxification in *Saccharomyces cerevisiae*.

The SEM images, EDX analysis coupled with the TEM and XRD analysis suggest that cadmium crystals were synthesized extracellularly by *P. chrysosporium*. Previous studies have shown an intimate association of extracellular proteins with spheroidal aggregates of biogenic metal nanocrystals [46]. Microbially derived extracellular proteins can limit the dispersal of biogenic nanoparticles and stabilize metal ions [47]. The complexation of heavy metals by extracellular polymeric substances and their precipitation on microbial cell surfaces could also protect the cells against heavy metal inhibition [48,49]. Therefore, the formation of cadmium crystal particles by *P. chrysosporium* is probably a detoxification mechanism to immobilize dissolved cadmium, and thus reduce its bioavailability and toxicity.

In summary, cadmium induces cellular death in some *P. chrysosporium* cells. The mechanism involves induction of mitochondrial cadmium toxicity with the breakdown of MMP and formation of ROS. ROS in turn induces plasma membrane damage. Some cells survive by activating antioxidant agents and biosynthesizing extracellular crystal particles to reduce the bioavailability and toxicity of cadmium. The results of this study might be useful for understanding the physiological responses of fungi exposed to environmental toxins. Further studies combining genomic/proteomic analysis and patch-clamp measurements are required to understand the genetic expression and signal transportation mechanism associated with these physiological responses.

Acknowledgments

This study was financially supported by the National Natural Science Foundation of China (51039001, 51378190, 51178171, 50908078), Program for New Century Excellent Talents in University (NCET-10-0361), the Hunan Provincial Natural Science Foundation of China (10JJ7005), the Scholarship Award for Excellent Doctoral Student granted by the Ministry of Education and the Research Fund for the Doctoral Program of Higher Education of China (20100161110012), the Hunan Provincial Innovation Foundation For Postgraduate (CX2012B137), Zhejiang Provincial Key Laboratory of Solid Waste Treatment and Recycling open fund (SWTR-2012-07).

Appendix A. Supplementary data

Supplementary data associated with this article can be found, in the online version, at doi:10.1016/j.procbio.2014.01.014.

References

[1] Fragoeiro S, Magan N. Enzymatic activity, osmotic stress and degradation of pesticide mixtures in soil extract liquid broth inoculated with *Phanerochaete chrysosporium* and *Trametes versicolor*. Environ Microbiol 2005;7:348–55.
[2] Huang DL, Zeng GM, Feng CL, Hu S, Jiang XY, Tang L, et al. Degradation of lead-contaminated lignocellulosic waste by *Phanerochaete chrysosporium* and the reduction of lead toxicity. Environ Sci Technol 2008;42:4946–51.
[3] Chen A, Zeng G, Chen G, Fan J, Zou Z, Li Hui, et al. Simultaneous cadmium removal and 2,4-dichlorophenol degradation from aqueous solutions by *Phanerochaete chrysosporium*. Appl Microbiol Biotechnol 2011;91:811–21.
[4] Boyle D. Effects of pH and cyclodextrins on pentachlorophenol degradation (mineralization) by white-rot fungi. J Environ Manage 2006;80:380–6.
[5] Chen G, Fan J, Liu R, Zeng G, Chen A, Zou Z. Removal of Cd(II), Cu(II) and Zn(II) from aqueous solutions by live *Phanerochaete chrysosporium*. Environ Technol 2012;33:2653–9.
[6] Huang DL, Zeng GM, Feng CL, Hu S, Zhao MH, Lai C, et al. Mycelial growth and solid-state fermentation of lignocellulosic waste by white-rot fungus *Phanerochaete chrysosporium* under lead stress. Chemosphere 2010;81:1091–7.
[7] Kiyono M, Miyahara K, Sone Y, Pan-Hou H, Uraguchi S, Nakamura R, et al. Engineering expression of the heavy metal transporter MerC in *Saccharomyces cerevisiae* for increased cadmium accumulation. Appl Microbiol Biotechnol 2010;86:753–9.
[8] Xu Q, Min H, Cai S, Fu Y, Sha S, Xie K, et al. Subcellular distribution and toxicity of cadmium in *Potamogeton crispus* L. Chemosphere 2012;89:114–20.
[9] Gallego SM, Pena LB, Barcia RA, Azpilicueta CE, Iannone MF, Rosales EP, et al. Unravelling cadmium toxicity and tolerance in plants: insight into regulatory mechanisms. Environ Exp Bot 2012;83:33–46.
[10] Sun J, Wang R, Zhang X, Yu Y, Zhao R, Li Z, et al. Hydrogen sulfide alleviates cadmium toxicity through regulations of cadmium transport across the plasma and vacuolar membranes in *Populus euphratica* cells. Plant Physiol Biochem 2013;65:67–74.
[11] Kim SJ, Jeong HJ, Myung NY, Kim M, Lee JH, So H, et al. The protective mechanism of antioxidants in cadmium-induced ototoxicity *in vitro* and *in vivo*. Environ Health Perspect 2008;116:854–62.
[12] Baldrian P. Interactions of heavy metals with white-rot fungi. Enzyme Microb Technol 2003;32:78–91.
[13] Li Q, Wu S, Liu G, Liao X, Deng X, Sun D, et al. Simultaneous biosorption of cadmium (II) and lead (II) ions by pretreated biomass of *Phanerochaete chrysosporium*. Sep Purif Technol 2004;34:135–42.
[14] Turk M, Plemenitaš A, Gunde-Cimerman N. Extremophilic yeasts: plasma-membrane fluidity as determinant of stress tolerance. Fungal Biol 2011;115:950–8.
[15] Kirk TK, Schultz E, Connors WJ, Lorenz LF, Zeikus JG. Influence of culture parameters on lignin metabolism by *Phanerochaete chrysosporium*. Arch Microbiol 1978;117:277–85.
[16] Perlin DS, Harris SL, Seto-Young D, Haber JE. Defective H^+-ATPase of hygromycin B-resistant *pma1* mutants from *Saccharomyces cerevisiae*. J Biol Chem 1989;264:21857–64.
[17] Aguilera F, Peinado RA, Millán C, Ortega JM, Mauricio JC. Relationship between ethanol tolerance, H^+-ATPase activity and the lipid composition of the plasma membrane in different wine yeast strains. Int J Food Microbiol 2006;110:34–42.
[18] Bradford MM. A rapid and sensitive method for the quantitation of microgram quantities of protein utilizing the principle of protein-dye binding. Anal Biochem 1976;72:248–54.
[19] Liang Y, Zhang W, Chen Q, Liu Y, Ding R. Effect of exogenous silicon (Si) on H^+-ATPase activity, phospholipids and fluidity of plasma membrane in leaves of salt-stressed barley (*Hordeum vulgare* L.). Environ Exp Bot 2006;57:212–9.

[20] Luo YH, Wu SB, Wei YH, Chen YC, Tsai MH, Ho CC, et al. Cadmium-based quantum dot induced autophagy formation for cell survival via oxidative stress. Chem Res Toxicol 2013;26:662–73.
[21] López E, Arce C, Oset-Gasque MJ, Cañadas S, González MP. Cadmium induces reactive oxygen species generation and lipid peroxidation in cortical neurons in culture. Free Radic Bio Med 2006;40:940–51.
[22] Choudhary M, Jetley UK, Khan MA, Zutshi S, Fatma T. Effect of heavy metal stress on proline, malondialdehyde, and superoxide dismutase activity in the cyanobacterium *Spirulina platensis*-S5. Ecotox Environ Safe 2007;66:204–9.
[23] Xiao X, Han Z, Chen Y, Liang X, Li H, Qian Y. Optimization of FDA–PI method using flow cytometry to measure metabolic activity of the cyanobacteria, *Microcystis aeruginosa*. Phys Chem Earth 2011;36:424–9.
[24] Li H, Feng T, Shi X, Liang P, Zhang Q, Gao X. Effects of pyrethroids and endosulfan on fluidity of mitochondria membrane in *Chilo suppressalis* (Walker). Pest Biochem Phys 2009;95:72–6.
[25] Braidot E, Petrussa E, Macrì F, Vianello A. Plant mitochondrial electrical potential monitored by fluorescence quenching of rhodamine 123. Biol Plantarum 1998;41:193–201.
[26] Tonshin AA, Saprunova VB, Solodovnikova IM, Bakeeva LE, Yaguzhinsky LS. Functional activity and ultrastructure of mitochondria isolated from myocardial apoptotic tissue. Biochemistry (Moscow) 2003;68:875–81.
[27] Zeng GM, Chen AW, Chen GQ, Hu XJ, Guan S, Shang C, et al. Responses of *Phanerochaete chrysosporium* to toxic pollutants: physiological flux, oxidative stress, and detoxification. Environ Sci Technol 2012;46:7818–25.
[28] Rehman A, Anjum MS. Multiple metal tolerance and biosorption of cadmium by *Candida tropicalis* isolated from industrial effluents: glutathione as detoxifying agent. Environ Monit Assess 2010;174:585–95.
[29] Li Q, McNeil B, Harvey LM. Adaptive response to oxidative stress in the filamentous fungus *Aspergillus niger* B1-D. Free Radic Biol Med 2008;44:394–402.
[30] Bai Z, Harvey LM, McNeil B. Physiological responses of chemostat cultures of *Aspergillus niger* (B1-D) to simulated and actual oxidative stress. Biotechnol Bioeng 2003;82:691–701.
[31] Hall JL. Cellular mechanisms for heavy metal detoxification and tolerance. J Exp Bot 2002;53:1–11.
[32] Astolfi S, Zuchi S, Passera C. Effect of cadmium on H^+ATPase activity of plasma membrane vesicles isolated from roots of different S-supplied maize (*Zea mays* L.) plants. Plant Sci 2005;169:361–8.
[33] Fodor E, Szabó-Nagy A, Erdei L. The effects of cadmium on the fluidity and H^+-ATPase activity of plasma membrane from sunflower and wheat roots. J Plant Physiol 1995;147:87–92.
[34] Morsy AA, Salama KHA, Kamel HA, Mansour MMF. Effect of heavy metals on plasma membrane lipids and antioxidant enzymes of *Zygophyllum species*. Eurasia J Biosci 2012;6:1–10.
[35] Janicka-Russak M, Kabala K, Burzynski M, Klobus G. Response of plasma membrane H^+-ATPase to heavy metal stress in *Cucumis sativus* roots. J Exp Bot 2008;59:3721–8.
[36] Acharya UR, Mishra M, Patro J, Panda MK. Effect of vitamins C and E on spermatogenesis in mice exposed to cadmium. Reprod Toxicol 2008;25:84–8.
[37] Prabu SM, Shagirtha K, Renugadevi J. Quercetin in combination with vitamins (C and E) improve oxidative stress and hepatic injury in cadmium intoxicated rats. Biomed Prev Nutr 2011;1:1–7.
[38] Gupta A, Jain DK, Shukla S, Shukla SK, Kumar S, Kumar S, et al. Amelioratives role of vitamin C, red cabbage extract (*Brassica oleracea*) and turmeric (*Curcuma longa*) rhizome extract alleviate cadmium-induced oxidative stress in freshwater bloch (*Heteropneustes fossilis*) in liver, gills and muscle. Int J Food Agric Vet Sci 2012;2:85–98.
[39] Garrido C, Galluzzi L, Brunet M, Puig PE, Didelot C, Kroemer G. Mechanisms of cytochrome c release from mitochondria. Cell Death Differ 2006;13:1423–33.
[40] Wang Y, Fang J, Leonard SS, Rao KMK. Cadmium inhibits the electron transfer chain and induces reactive oxygen species. Free Rad Biol Med 2004;36:1434–43.
[41] Dhir B, Sharmila P, Saradhi PP. Hydrophytes lack potential to exhibit cadmium stress induced enhancement in lipid peroxidation and accumulation of proline. Aquat Toxicol 2004;66:141–7.
[42] Letelier ME, Lepe AM, Faúndez M, Salazar J, Marín R, Aracena P, et al. Possible mechanisms underlying copper-induced damage in biological membranes leading to cellular toxicity. Chem Biol Interact 2005;151:71–82.
[43] Basha PS, Rani AU. Cadmium-induced antioxidant defense mechanism in freshwater teleost *Oreochromis mossambicus* (Tilapia). Ecotoxicol Environ Safe 2003;56:218–21.
[44] Matsufuji Y, Yamamoto K, Yamauchi K, Mitsunaga T, Hayakawa T, Nakagawa T. Novel physiological roles for glutathione in sequestering acetaldehyde to confer acetaldehyde tolerance in *Saccharomyces cerevisiae*. Appl Microbiol Biotechnol 2013;97:297–303.
[45] Gharieb MM, Gadd GM. Role of glutathione in detoxification of metal(loid)s by *Saccharomyces cerevisiae*. BioMetals 2004;17:183–8.
[46] Moreau JW, Weber PK, Martin MC, Gilbert B, Hutcheon ID, Banfield JF. Extracellular proteins limit the dispersal of biogenic nanoparticles. Science 2007;316:1600–3.
[47] Sanghi R, Verma P. Biomimetic synthesis and characterisation of protein capped silver nanoparticles. Bioresour Technol 2009;100:501–4.
[48] Yang Y, Mathieu JM, Chattopadhyay S, Miller JT, Wu T, Shibata T, et al. Defense mechanisms of *Pseudomonas aeruginosa* PAO1 against quantum dots and their released heavy metals. ACS Nano 2012;6:6091–8.
[49] Sheng GP, Xu J, Luo HW, Li WW, Li WH, Yu HQ, et al. Thermodynamic analysis on the binding of heavy metals onto extracellular polymeric substances (EPS) of activated sludge. Water Res 2013;47:607–14.